# Reaction to fire of polymethylmethacrylate and polyvinylchloride under reduced oxygen concentrations in a controlled-atmospherecone calorimeter

Sarah Chatenet, Olivier Authier, Serge Bourbigot, Gaëlle Fontaine

▶ **To cite this version:**

## HAL Id: hal-03658599
## https://hal.univ-lille.fr/hal-03658599v1

# Page Proof Instructions and Queries

Thank you for choosing to publish with us. This is your final opportunity to ensure your article will be accurate at publication. Please review your proof carefully and respond to the queries using the circled tools in the image below, which are available in Adobe Reader DC* by clicking **Tools** from the top menu, then clicking **Comment**.

Please use *only* the tools circled in the image, as edits via other tools/methods can be lost during file conversion. For comments, questions, or formatting requests, please use T̲ . Please do *not* use comment bubbles/sticky notes ⊜.



*If you do not see these tools, please ensure you have opened this file with **Adobe Reader DC**, available for free at get.adobe.com/reader or by going to Help > Check for Updates within other versions of Reader. For more detailed instructions, please see us.sagepub.com/ReaderXProofs.

| Sl. No. | Query |
| --- | --- |
| | Please note that we cannot add/amend ORCID iDs for any article at the proof stage. Following ORCID's guidelines, the publisher can include only ORCID iDs that the authors have specifically validated for each manuscript prior to official acceptance for publication. |
| | Please confirm that all author information, including names, affiliations, sequence, and contact details, is correct. |
| | Please review the entire document for typographical errors, mathematical errors, and any other necessary corrections; check headings, tables, and figures. |
| | Please ensure that you have obtained and enclosed all necessary permissions for the reproduction of artworks (e.g. illustrations, photographs, charts, maps, other visual material, etc.) not owned by yourself. Please refer to your publishing agreement for further information. |
| | Please note that this proof represents your final opportunity to review your article prior to publication, so please do send all of your changes now. |
| | Please Confirm That The Funding and Conflict of Interest Statements are Accurate. |
| 1 | Please provide complete postal address with zip code for the affiliation details of the corresponding author. |
| 2 | Please provide a 2- to 3-sentence biography for each of the authors. |
| 3 | Please provide date of report (if any) for Ref. 2. |
| 4 | Please provide complete reference details for Ref. 18. |
| 5 | Please provide the page range for Ref. 22. |
| 6 | Please provide date of report (if any) for Ref. 34. |

# Reaction to fire of polymethylmethacrylate and polyvinylchloride under reduced oxygen concentrations in a controlled-atmosphere cone calorimeter

**Sarah Chatenet[1], Olivier Authier[1]** (ID)**, Serge Bourbigot[2]** (ID)
**and Gaëlle Fontaine[2]** (ID)

## Abstract
Electrical cable sheaths are the most abundant fire load in nuclear power plants, mainly in rooms that are kept in under slight pressure. This configuration leads fires to grow in under-ventilated and vitiated conditions. Assessing fire threat involves characterizing the heat released, responsible for fire growth, and the smoke evolved, which may interact with sensitive components in the area. For that purpose, a revisited controlled-atmosphere cone calorimeter has been designed, set up, and coupled to a Fourier transformed infrared spectrometer and an electrical low-pressure impactor to measure simultaneously the evolved gases and aerosols, respectively. This bench-scale apparatus has been first qualified with polymethylmethacrylate. It has second been used to characterize polyvinylchloride cable sheath representative material reaction to fire in under-ventilated and vitiated conditions. It appeared that vitiation in under-ventilated fires lowers the heat release rate and the fuel mass loss rate.

[1]EDF R&D, Chatou, France
[2]Ecole Nationale Supérieure de Chimie de Lille, Unité Matériaux et Transformations, Villeneuve-d'Ascq, France[AQ: 1]

**Corresponding author:**
Gaëlle Fontaine, Ecole Nationale Supérieure de Chimie de Lille, Unité Matériaux et Transformations, Villeneuve-d'Ascq, France.
Email: gaelle.fontaine@centralelille.fr

## Introduction

In the nuclear industry for power generation, fire is frequent internal aggression with an occurrence of one fire outbreak per year and per nuclear unit in France. A fire is threatening by two means: the heat released that may drive fire growth and smoke evolution. Smoke is composed of gases and aerosols that may be transported away from the start of the fire and interact with components in the area. In nuclear power plants (NPPs), compartments in the buildings are generally sealed from one to another while connected to a ventilation network. This ventilation system provides a suitable pressure cascade to prevent any accidental radio-active leak within the compartment from escaping into the atmosphere. The compartments containing radioactive materials are under-pressurized and the outgoing airflows are gathered and filtered thanks to high-efficiency air-cleaning devices.[1] As flaming fires consume the oxygen, this low ventilation level drives confined fires under oxygen-depleted conditions (i.e. $(O_2) < 21$ vol. %) at advanced stages. On the one hand, the fire is under-ventilated when the airflow rate is less than the amount required for complete combustion (ventilation-controlled combustion, e.g. due to limited ventilation openings). On the other hand, the fire is vitiated when the oxygen concentration in the inlet gas flow can range from 21 vol. % down to 0 vol. %. It can typically result from the mixing of the smoke within the enclosure, or from ventilation conditions where oxygen is gradually consumed and replaced by combustion products. As NPPs can require more than 1600 km of electrical cable, electrical cable sheaths are the most abundant fire load in these premises.[2] In all the running NPPs, which are second-generation NPPs, electrical cable sheaths are mainly polyvinylchloride (PVC)-based formulated materials. To assess the consequence of an NPP fire, experimental studies at laboratory scale are particularly crucial in under-ventilated and vitiated conditions.

Different designs of controlled-atmosphere cone calorimeter (CACC) have been set up in laboratories[3–15] to study the flammability parameters of various polymers, for example, polymethylmethacrylate (PMMA), polyethylene (PE), polypropylene (PP), or polystyrene (PS), as well as the smoke produced by under-ventilated and vitiated fires. The tests in CACC imply that phenomena can be controlled by both ventilation and vitiation of the gas supply. Apparatus with a sealed connection between a controlled-atmosphere enclosure and the ductwork is titled closed CACC, while those having an open connection between the controlled-atmosphere chamber and the exhaust duct are titled open CACC.[3] Bench-scale testing involves samples in the range of grams to kilograms submitted to a constant and calibrated radiative heating source which leads the sample to behave representatively of a real fire at a chosen stage. During the test, the condensed phase and the gas phase are not separated so the self-maintained phenomenon of combustion is represented. The fire propagation apparatus (FPA) was designed in the mid-1970s under the direction of A. Tewarson. It was standardized as ISO 12136:2011[16] and ASTM E2058.[4] The cone calorimeter in its open version was developed in the early 1980s at the National Bureau of Standards by V. Babrauskas. It was standardized as ISO 5660-1:2015[5] and ASTM E1354.[6] The National Institute of Standard and Technology (NIST) developed a CACC in 1992.[7] In addition to the CACC apparatus, the Purser furnace apparatus also enables different fire stages to be created.[17] The operation of the open CACC has been recently standardized with ISO 5660-5:2020.[8] However, the experimental work presented in this study has been conducted before the publication of ISO 5660-5 in 2020. Therefore, our results cannot be based on this standard. There are a few variations in our apparatus[18] and the designs described by ISO 5660-5 or other researchers. Our CACC apparatus allows us to perform fire tests in under-

ventilated and vitiated conditions to get complementary data to observation obtained in the well-known ventilated regime.

The tests conducted in these benches have shown that the mass loss rate (MLR),[19–22] heat release rate (HRR), and total heat release[21,22] decrease when vitiation increases. The carbon monoxide yield[21,23] and the soot yield[23] increase. The total flame radiation and the emittance decrease, whereas the flame temperature remains constant.[20] Time to ignition remains unchanged when vitiation increases.[22] When the equivalence ratio increases in under-ventilation conditions, the MLR decreases for some studies[23–25] and remains constant for others,[22,26] the heat release rate decreases,[22,27,28] the convective fraction efficiency decreases, whereas the radiative fraction efficiency has a gaussian shape.[27] The soot yield increases for most studies[25,27] but remains constant in another study.[28] The carbon monoxide yield increases and the carbon dioxide yield decreases[25,27–29] and gas temperature decreases.[25] Low molecular weight hydrocarbons yield increases.[27,29] However, a lack of data on PVC materials under CACC conditions can be underlined.

A bench-scale apparatus in which small plaques are subjected to a radiative heat flux of 50 kW/m$^2$ has been designed allowing us to characterize simultaneously the fire parameters, that is, HRR and MLR, and the smoke, that is, the light gases and the aerosols. This apparatus is designed to study the inlet flow rate and the oxygen concentration over a wide range of conditions. It consists of a new design of CACC coupled to a Fourier transformed infrared (FTIR) spectrometer and an electrical low-pressure impactor (ELPI) particle sizer. Two unique features can be highlighted: the gas mixture is distributed in a very homogeneous way at the inlet before mixing with pyrolysis gases, and additional sampling connections included in the chimney are used for measuring temperature and collecting gases and aerosols before analysis by various techniques. Previous results to investigate the fire behavior of ethylene vinyl acetate (EVA) and EVA/ATH (with aluminum trihydroxide) using the open mass loss cone/FTIR/ELPI are reported by Ngohang and colleagues.[30–32] Since PMMA is a widely studied material in the fire science field, tests with PMMA are first carried out on the new apparatus to compare with the literature. In a second time, the same tests with PVC cable sheath representative material are performed.

## Material and methods

### Methods

*Bench overview.* A CACC was designed to fulfill the following requirements:

- Controlling confinement and the atmosphere composition between 2% and 21 vol. % as well as the inlet flow rate between 0 and 200 L/min;
- Getting a reliable HRR measurement in under-ventilated combustion under an applied heat flux of 50 kW/m$^2$, representative of mid to advanced fires;
- Ensuring a dispersion of the gas mixture at room temperature within the enclosure (i.e. horizontally homogeneous flow velocity);
- Allowing a transmission of the infrared emission coming from the flame to avoid additional local heating;

- Allowing good visibility of the sample burning;
- Allowing the instrumentation of mass loss, heat release rate, gas concentration, and aerosols concentration to be performed.

Figure 1 displays an overview of the apparatus and specific elements are detailed subsequently. The airtight enclosure ($60 \times 60 \times 60$ cm$^3$) is composed of stainless steel 316 L framework on which four windows made of polycarbonate are silicon-sealed (surface ratio of windows over the framework of 80% vs 20%). The heater element is wound in the form of a truncated cone rated 4200 W at 230 V with a radiative heat output of up to 75 kW/m$^2$. Its temperature is controlled by 3 K-type thermocouples embedded inside the spires. A flux meter (OP837193 supplied by Captec) is used to evaluate the heat flux delivered by the conical resistance. A one-piece shutter made of an insulating ceramic fiber element laid on a stainless-steel round plate is used to protect the sample from the heat flux before beginning the test. The sample is positioned on a stainless-steel plate ($10 \times 10$ cm$^2$) which is directly placed on a refractory firebrick. The load cell used for measuring mass has a sample capacity of over 500 g (accuracy of 0.01 g). The spark igniter used to pilot the ignition provides a tension of 10 kV between its two electrodes. The chimney provided by FTT is a 0.6-m-high cylinder with a 0.12-m diameter. The flow regime in the chimney is intermediate to turbulent according to the Reynolds number (~3000) used to predict the transition from laminar to turbulent flow, which favors radial mixing and homogeneous flow. In comparison to the standardized apparatus, additional sampling connections are used upstream of the mixing of the smoke with the ambient air, for measuring temperature and collecting gases and aerosols before analysis by various techniques. Thus, an extra part (150 mm) on the top of the chimney is instrumented with three sampling lines, four K-type thermocouples, and a flow velocity sensor (L Pitot tube CP211HOR supplied by Kimo, accuracy of 0.5%). Sampling connections included in the chimney are positioned a few centimeters from the smoke exhaust. A regulation system is used to mix and deliver a controlled mixture of dry air and nitrogen (purity: 95%–99.9999%) at room temperature and a flow rate between 30 and 120 L/min. The mixture is distributed under a 10-mm-thick sintered stainless-steel plate creating a pressure drop of 0.1 bar (supplier: Poral). A zirconium oxygen controller (supplied by Buhler under the reference BA 1000) is used to measure the $O_2$ concentration inside the enclosure. Its range of measurement is from 0.1 up to 25 vol.% with an accuracy of 2% and a response time of 3 s. A paramagnetic oxygen sensor (Servomex Servopro 4900) is used to measure the $O_2$ concentration in smoke from 0% to 25 mol.% with an accuracy of 0.5% and a response time of 15 s, with a gas sampling of 1 L/min and after $H_2O$ removing by a cooling unit and a moisture sorbent. In smoke, light gases, that is, substances at a gaseous state at 180°C, are measured continuously with FTIR and aerosols, that is, soot and condensed hydrocarbons, are measured continuously with an ELPI.

*Heat release rate measurement.* HRR is calculated according to equation (1) after Huggett's[33] law and its assumptions made by Parker[34] and Janssens.[35] Thus, HRR is obtained from the measurement of $O_2$, CO, and $CO_2$ concentrations in the gas phase and the mass flow rate of the incoming stream.

Equation (1): HRR calculation taking into account the amount of carbon dioxide and carbon monoxide released
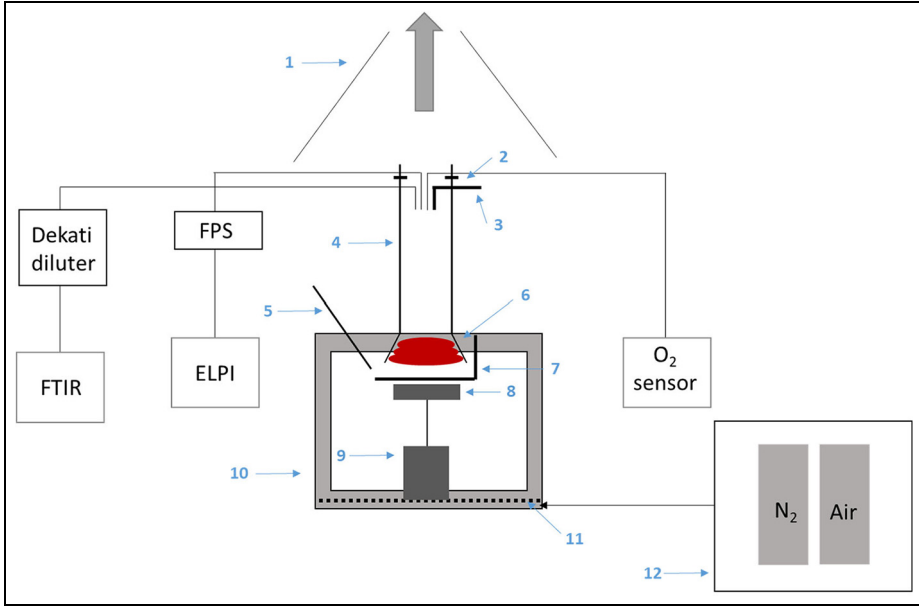
**Figure 1.** Overview of the apparatus developed.
1: Air extraction, 2: Thermocouples, 3: Flow velocity sensor, 4: Chimney, 5: Zirconium oxygen sensor, 6: Heater, 7: Movable shutter, 8: Sample holder, 9: Load cell, 10: Enclosure, 11: Sintered stainless-steel plate, 12: Gas mixing board.

$$\dot{q} = 10^3 \left[ E \frac{X_{O_2}^0(1 - X_{CO_2} - X_{CO}) - X_{O_2}\left(1 - X_{CO_2}^0\right)}{1 - X_{O_2} - X_{CO_2} - X_{CO}} - (E_{CO} - E)\frac{X_{CO}\left(1 - X_{O_2}^0 - X_{CO_2}^0\right)}{2(1 - X_{O_2} - X_{CO_2} - X_{CO})} \right]$$

$$\dot{m}_a \frac{M_{O_2}}{M_a}\left(1 - X_{H_2O}^0\right)$$

$$\tag{1}$$

where $\dot{q}$ is the heat release rate (kW), $E$ is the Huggett constant ($=13.1$ MJ/kg of $O_2$ consumed), $X_{O_2}^0$ is the mole fraction of $O_2$ in the incoming stream, $X_{CO_2}^0$ is the mole fraction of $CO_2$ in the incoming stream (assumed to be negligible, e.g. $\sim 410$ ppmv in air), $M_{O_2}$ is the molecular weight of $O_2$ ($32 \times 10^{-3}$ kg/mol), $M_{N_2}$ is the molecular weight of nitrogen ($28 \times 10^{-3}$ kg/mol), $X_{O_2}$, $X_{CO_2}$, and $X_{CO}$ are the mole fractions of, respectively, $O_2$, $CO_2$, and CO in the exhaust stream, $E_{CO}$ is the net heat release per unit mass of $O_2$ consumed for combustion of CO to $CO_2$ ($=17.6$ MJ/kg of $O_2$), $\dot{m}_a$ is the mass flow rate of the incoming stream (kg/s), $M_a$ is the molecular weight of the incoming stream ($28.97 \times 10^{-3}$ kg/mol in the case of air), and $X_{H_2O}^0$ is the mole fraction of $H_2O$ in the incoming stream, assumed to be around 0 as the incoming air is primarily dried.

*FTIR spectrometer.* A Thermo Nicolet iS10 FTIR spectrometer equipped with a nitrogen Mercury Cadmium Telluride (MCT) detector, 0.2 L volume gas cell, and 2 m optical path length, was set. Acquisitions were performed in mid-infrared (from 4100 to 650 cm$^{-1}$) with

high-spectral resolution (set at 0.5 cm$^{-1}$) and a scan number of one to get a real-time analysis (each scan was taken at 1.61 s and 0.5 cm$^{-1}$ as spectral resolution). The number of scans used for the acquisition of quantitative calibration gases was set at 20 to enhance the signal/noise ratio. The polytetrafluoroethylene (PTFE) gas transport line and the FTIR gas cell are heated at 180°C to avoid condensation of volatiles. A pump (equipped with a flow meter and valve) to get controlled and constant flow (3.5 L/min) was put after the FTIR spectrometer and a pressure gauge with regulating valve to keep constant pressure (650 ± 5 Torr) was set into the gas cell. Each gas ($CO_2$, $CO$, $H_2O$, $CH_4$, $C_2H_4$, $C_2H_2$, $C_6H_6$, and $HCl$) was calibrated in this study using the Classical Least Square (CLS) algorithm as an FTIR gas computing model and considering all the unavoidable interferences between substances.[30–32] Dilution of smoke is performed upstream the FTIR spectrometer in the CACC configuration to get into the gas's calibration range thanks to a Dekati Diluter.

*ELPI particle sizer.* Cascade impactors are widely used to measure particle size distributions in a variety of applications. An ELPI from Dekati is used to measure in real-time the size distribution and the concentration of aerosols.[36] The operating principle of the ELPI can be summarized in three consecutive steps. First, particles sampled from smoke are exposed to a unipolar positive ion environment in the corona charger, where they are electrically charged to a known charge level. In the second step, the charged particles enter the low-pressure cascade impactor where they are classified into size fractions of 6 nm to 10 μm according to their aerodynamic diameter, the latter determining their deposition at a particular ELPI stage. In the final step, charges carried by particles are continuously measured, at each impactor stage, by sensitive electrometers located inside the ELPI and the measured current values are inverted to yield particles' number (per cm$^3$) using transfer functions provided by manufacturers. The antistatic PTFE ELPI sampling line was heated at 180°C to prevent effects of condensed humidity on the measurement. A vacuum pump located at the far side of the ELPI is set by the manufacturer to regulate isokinetic flow to a rate of 10 L/min. Dilution of smoke is performed upstream the ELPI particle sizer thanks to an FPS-4000 from Dekati. In practice, the ELPI enables detection of particles with a 15-stage low-pressure cascade impactor, including 14 impactor stages (contains one precut stage to remove large particles, not measured electrically) plus a final filter (also connected to the electrometer) that collects in the last stage the particles too small to be deposited by impaction in the previous stages. Particles are finally classified into 14 size fractions on the impactor according to their aerodynamic diameter.

## Materials

The representative material of PVC cable sheath is made of a simplified formulation made of 38.3 wt. % of PVC, 28.3 wt. % of diisodecylphthalate (DIDP), 31.4 wt. % of calcium carbonate ($CaCO_3$) and 1.9 wt. % of Ca/Zn thermal stabilizer. In this formulation, the PVC, referenced as "PVC Lacovyl S 7015-PCC 016VPT," is provided by Kem One. The DIDP, referenced as "Jayflex" is provided by Caldic. The $CaCO_3$, referenced as "EHX1 OM," is provided by OMYA. The Ca/Zn thermal stabilizer is a one-pack compound provided by ChemTech. The formulation was mixed in a CP 200 L high-speed mixer from

CACCIA. Neat PVC is first introduced in the mixer and rapidly heats to 80°C. The additives are slowly added before rapid increase of the temperature to 110°C. The formulation is then transferred into a cold tank and the obtained "dry-blend" is conditioned at 25°C in PE bags. The formulation is injection-molded and heated up to 200°C in the form of plaques of $100 \times 100 \times 3$ $mm^3$.

Neat and transparent PMMA is provided by Goodfellow under the reference ME303050 and cut in the shape of $100 \times 100 \times 5$ $mm^3$ plaques.

### Fire testing

Sample plates of PVC-based formulation and PMMA placed in a horizontal orientation in the CACC holder were tested under 50 kW/m² and different $O_2$ concentrations of 21, 18, 16, 13, 9, 6, and 2 vol. % with a low-ventilation rate of 30 L/min in the enclosure to simulate an advanced stage confined fire, as specified in the ISO 19706:2011[37] classification of fire stages.

The $[CO]/[CO_2]$ ratio is used in our study to choose the inlet flow rate to be used under controlled-atmosphere conditions. The $[CO]/[CO_2]$ ratio is inferior to 0.05 for well-ventilated flaming fires. For confined under-ventilated flaming fires, the $[CO]/[CO_2]$ ratio is comprised between 0.2 and 0.4.[37] In addition, the ventilation conditions and fire stages are commonly characterized by the global equivalence ratio[11,38] defined as the mass ratio of the actual fuel/air ratio to the stoichiometric fuel/air ratio for complete combustion. If the amount of air equals the fuel-air requirement, then the conditions are stoichiometric, and the equivalence ratio equals 1. If the equivalence ratio is higher, then the conditions are defined as ventilation-controlled combustion, and if the air requirement is exceeded, then the conditions are well-ventilated. The chosen inlet volume airflow rate of 30 L/min, close to the values used by Tewarson and Pion,[19] provides confined under-ventilated combustion for both materials, that is, low air supply and fuel-rich flame, on both the $[CO]/[CO_2]$ and equivalence ratio criteria. Indeed, the $[CO]/[CO_2]$ ratio varies during the tests between 0.1 and 0.3 and the equivalence ratio is globally between 1 and 4, using the stoichiometric mass air-to-fuel ratio of 8.27 for PMMA and 8.42 for filled PVC.

### Data processing and repeatability

For each experiment under the same conditions, at least three runs were carried out. Data are processed with the aim to consider the experimental uncertainties and the repeatability. To do so, an average curve, that is, the arithmetic average at each time for all the runs, as well as the standard deviation associated, is calculated. The run curve that has the minimum difference with the calculated average curve is chosen as the "reference." The standard deviation based on the different runs is plotted on the same graph around the average curve which is not displayed to keep the figure clear and readable. Furthermore, the transfer time, that is, the mean residence time from the sample to the different analysis tools, is subtracted from the measured time before plotting the data on the figures of HRR, gases, and aerosols. Transfer times, around 10 s, were estimated by matching flame markers ($CO_2$, $H_2O$, and $O_2$) with time to ignition.

**Table 1.** Evolution of fire parameters with the $O_2$ content for PMMA testing.

| $O_2$ content (vol. %) | TTI (s) | TTE (s) | Residue (%) | pMLR (g/s) | pHRR (kW/m$^2$) | THR (MJ/m$^2$) |
|---|---|---|---|---|---|---|
| **21**_Std Deviation_ | 22.70.6 | 366.724.6 | 00 | 0.2840.005 | 488.93.9 | 129.80.8 |
| **18**_Std Deviation_ | 34.32.1 | 3937 | 00 | 0.2640.009 | 450.539.7 | 126.51.1 |
| **16**_Std Deviation_ | 40.616.5 | 42618.4 | 00 | 0.2460.003 | 385.713.6 | 113.23.1 |
| **13**_Std Deviation_ | 43.318.6 | 475.518.6 | 00 | 0.2230.005 | /* | /* |
| **9**_Std Deviation_ | / | / | 00 | 0.1800.004 | / | / |
| **6**_Std Deviation_ | / | / | 00 | 0.1730.002 | / | / |
| **2**_Std Deviation_ | / | / | 00 | 0.1750.009 | / | / |

PMMA: polymethylmethacrylate; THR: total heat release; TTE: time to extinction; TTI: time to ignition.

## Results

### Effect of vitiation on fire parameters

*Observations.* When lowering the oxygen content in the inlet gas stream injected at room temperature, it is observed a critical oxygen limit underneath which the flame is quenched. This threshold is about 13 vol. % for PMMA materials and about 15 vol. % for PVC-based materials.

Normalized mass and MLR of PMMA versus time at different $O_2$ contents in the inlet gas stream (2, 6, 9, 13, 16, 18, and 21 vol. %) are plotted in Figure 2(a) and (b), respectively. It is observed that PMMA leaves no residue after thermal decomposition regardless of the $O_2$ content in the inlet gas stream (Figure 2(a)). Also, the onset time of thermal decomposition, as well as the time to ignition (TTI) and the time to extinction (TTE), increases when the $O_2$ content decreases (Table 1). The increase in the TTI with the decrease in $O_2$ content was also observed in Christy et al.[22] Figure 2(b) shows that the peak of mass loss rate (pMLR) decreases when the $O_2$ content decreases in the flaming mode. Between 21 and 13 vol. % of $O_2$, pMLR decreases from 0.284 to 0.223 g/s ($-21\%$). However, pMLR remains constant, around 0.175 g/s, when the $O_2$ content decreases in the nonflaming mode from 9 to 2 vol. % of $O_2$.

In Figure 3, the HRR of PMMA at different $O_2$ contents (from 16 to 21 vol. %) is plotted. When the $O_2$ content decreases from 21 to 16 vol. %, the peak of heat release rate (pHRR) decreases from 489 to 386 kW/m$^2$ ($-20\%$) and the total heat release (THR) decreases from 130 to 113 MJ/m$^2$ ($-13\%$). The stabilization step after ignition is more noticeable for the HRR than for the MLR. Two factors may explain the differences in profiles over time between MLR and HRR, especially for the HRR: the residence time distribution in the gas phase and the response times of instruments used to measure CO, $CO_2$, and $O_2$ concentrations. To improve the dynamic HRR measurement based notably on CO, $CO_2$, and $O_2$ concentrations in the gas phase, the residence time distribution in the gas phase should be characterized in more detail than the mean residence time, defined as the ratio of pipe volume to volume flow, to obtain complete hydrodynamic data and help for improvement of data processing. In addition, the response times related to mass measurement using load cell are shorter than those of instruments measuring gas concentrations and flow velocity (response time up to 15 s using the paramagnetic sensor), which may also contribute to the difference in shape between MLR and HRR.
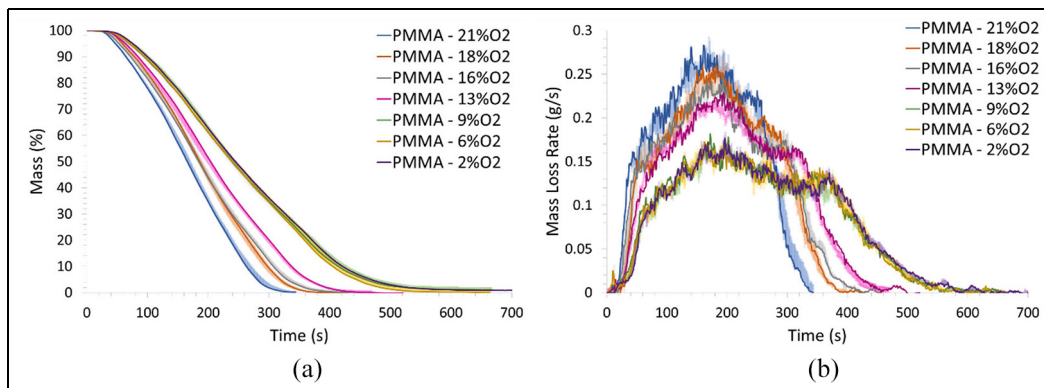
**Figure 2.** Evolution of mass of PMMA at different $O_2$ contents in the inlet gas stream (a) normalized mass and (b) mass loss rate.
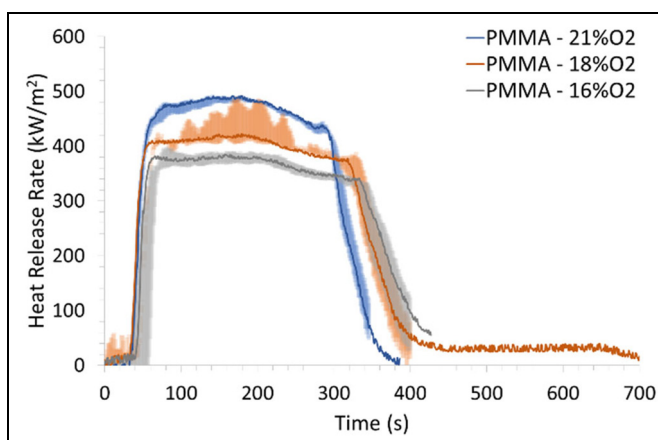PMMA: polymethylmethacrylate.



**Figure 3.** HRR of PMMA combustion at different $O_2$ contents in the inlet gas stream.
HRR: heat release rate; PMMA: polymethylmethacrylate.

The normalized mass and MLR of filled PVC as a function of time at different $O_2$ contents in the inlet gas stream (2, 6, 9, 16, 18, 21 vol. %) are plotted as shown in Figure 4(a) and (b), respectively. Figure 4(a) shows that the amount of filled PVC residue after thermal decomposition increases when the $O_2$ content decreases from 36.7% at 21 vol. % $O_2$ to 40.4% at 2 vol. % $O_2$. This result is consistent with the reduced oxidation of char at lower $O_2$ concentrations. The onset time of filled PVC thermal decomposition, as well as the TTI (Table 2), is independent of the $O_2$ content. Figure 4(b) shows that the pMLR decreases when the $O_2$ content decreases in the flaming mode. Between 21 and 16 vol. % of $O_2$, pMLR is decreased by 17%. However, pMLR remains constant at around 0.076 g/s when the $O_2$ content decreases in the nonflaming mode between 9 and 2 vol. % of $O_2$.

**Table 2.** Evolution of fire parameters with the $O_2$ content for filled PVC testing.

| $O_2$ content (vol. %) | TTI (s) | TTE (s) | Residue (%) | pMLR (g/s) | pHRR (kW/m$^2$) | THR (MJ/m$^2$) |
|---|---|---|---|---|---|---|
| **21** *Std Deviation* | 23.3 2.1 | 62 1.0 29.5 | 36.7 0.7 | 0.129 0.009 | 226 5.4 | 46.1 1.1 |
| **18** *Std Deviation* | 22.7 0.6 | 63 1.6 13.2 | 37.1 0.1 | 0.125 0.006 | 340.3 37.6 | 74.6 11.2 |
| **16** *Std Deviation* | 23.7 1.2 | 64 2.7 22.7 | 37.7 0.5 | 0.107 0.007 | 311 12.2 | 73.3 5.1 |
| **9** *Std Deviation* | / | / | 38.9 0.3 | 0.079 0.004 | / | / |
| **6** *Std Deviation* | / | / | 40.3 0.4 | 0.076 0.005 | / | / |
| **2** *Std Deviation* | / | / | 40.4 0.5 | 0.076 0.001 | / | / |

pHRR: peak of heat release rate; pMLR: peak of mass loss rate; PMMA: polymethylmethacrylate; PVC: polyvinylchloride; THR: total heat release; TTE: time to extinction; TTI: time to ignition.
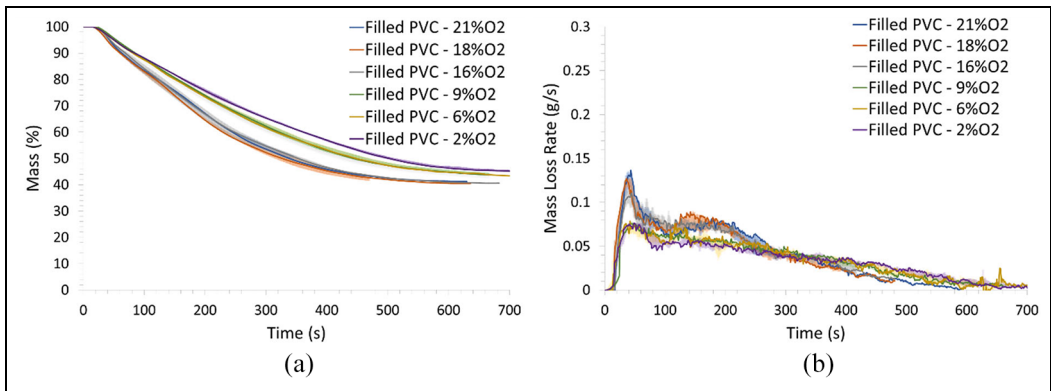


**Figure 4.** Evolution of mass of filled PVC at different $O_2$ contents in the inlet gas stream (a) normalized mass and (b) mass loss rate.
PVC: polyvinylchloride.

In Figure 5, the HRR of unfilled PVC at different $O_2$ contents (from 16 to 21 vol. %) is plotted. When the $O_2$ content decreases from 21 to 16 vol. %, pHRR and THR do not show any trend variation (within the 10% margin error).

The equivalence ratios over time are given in Figure 6 for both materials. For the PMMA case around the pMLR, that is, at approximately 180 s, the equivalence ratio varies from 3.8 at 21 vol. % $O_2$ to 2.9 at 13 vol. % $O_2$. For the filled PVC case around the pMLR, that is, at approximately 50 s, the equivalence ratio varies from 1.8 at 21 vol. % $O_2$ to 1.5 at 16 vol. % $O_2$. Thus, the fire regime is then still under-ventilated on the equivalence ratio criterion regardless of the $O_2$ content.

*Discussion.* Figure 7(a) and (b) shows the variation of the normalized pMLR with the $O_2$ content for PMMA and filled PVC, respectively. The dots represent normalized pMLR average values (pMLR values from Tables 1 and 2, at each $O_2$ content by the corresponding value in normal $O_2$ content, i.e. at 21 vol. %) and their respective standard deviations are represented by y—error bars.
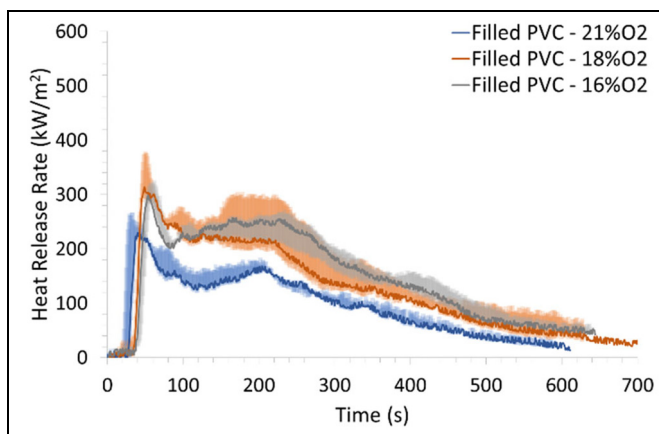
**Figure 5.** HRR of filled PVC combustion at different $O_2$ contents in the inlet gas stream.
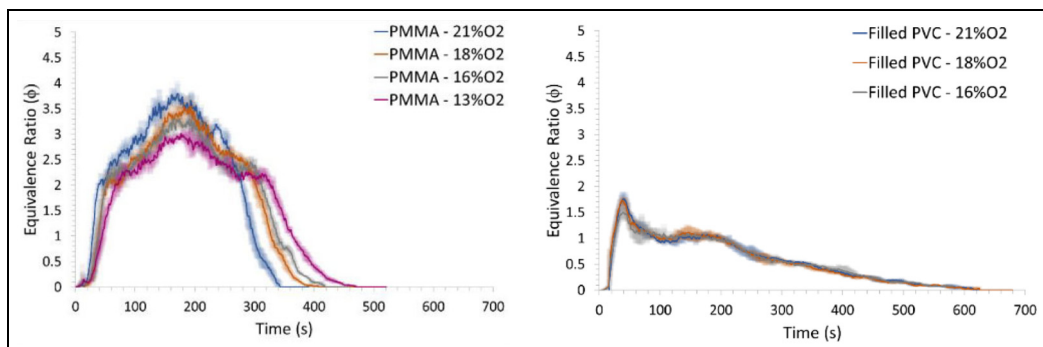HRR: heat release rate; PVC: polyvinylchloride.



**Figure 6.** Evolution of equivalence ratio during PMMA (left) and filled PVC (right) burning at different $O_2$ contents in the inlet gas stream.
PMMA: polymethylmethacrylate; PVC: polyvinylchloride.

In the flaming mode, pMLR decreases linearly when the $O_2$ content decreases for the three materials, whereas in the nonflaming mode, pMLR remains relatively constant when the $O_2$ content decreases. Once the flame is set, an additional radiative heat flux is applied to the material. The value of this heat flux is estimated at around 15 kW/m$^2$ for PMMA well-ventilated fires in the cone calorimeter.[39] This has the effect of increasing the material decomposition rate. As stated in Tewarson et al.,[40] a lower $O_2$ content strongly decreases the PMMA flame temperature and the combustion efficiency. The additional radiative heat flux received by the PMMA condensed phase is then decreased. On the other hand, the effect of $O_2$ depletion on the condensed phase thermal decomposition has no effect since when a diffusion flame is present, the region above the condensed phase surface is deprived of $O_2$ as the $O_2$ is consumed by the flame.[41,42]
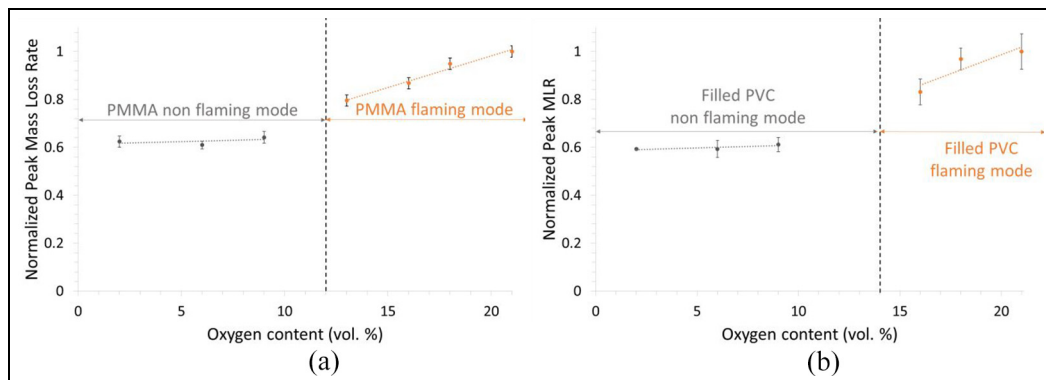
**Figure 7.** Normalized peak of mass loss rate versus the $O_2$ content for (a) PMMA, (b) unfilled PVC, and (c) filled PVC.
PMMA: polymethylmethacrylate; PVC: polyvinylchloride.

However, in the nonflaming mode, oxygen may have a direct effect on the condensed phase of the decomposing PMMA because of thermo-oxidative reactions. Though, the experimental results show that $O_2$ has no significant effect on the thermal decomposition rate of PMMA and filled PVC. It may be explained by the fact that at high irradiance exposure such as 50 kW/m², the gaseous products emission phenomenon resulting from in-depth thermolysis reactions overcomes the $O_2$ diffusion phenomenon inside the PMMA material.[26] Then, the oxidative reactions occur only at the surface of the material and, as a result, are not significant to the decomposition rate.

The decrease of PMMA flame radiation in vitiated atmospheres has been highlighted in Santo and Tamanini,[20] and the same observations regarding the dependence of pMLR and pHRR toward the $O_2$ content with PMMA are found in the literature.[20–22,26] A comparison of the present work experimental values of pMLR and pHRR versus $O_2$ content for PMMA with the mentioned bibliographic references values is made in Figure 8(a) and (b), respectively. In the flaming mode, the PMMA pMLR decreases linearly with the $O_2$ content. All the studies that experimented the effect of vitiation with PMMA submitted to a 50 kW/m² radiative heat flux give approximately the same slope in the pMLR decrease. The same study with a radiative heat flux of 30 kW/m² gives a higher slope in the decrease of pMLR with the $O_2$ content variation in the flaming mode. All of the data gathered regarding the influence of vitiation in the nonflaming mode indicate that there is no influence of the $O_2$ content on pMLR. A few studies are dedicated to the effect of vitiation on the pHRR. Among the two studies reported in Figure 8(b) and the present work, all of the three series of data indicate that pHRR decreases also linearly with the $O_2$ content and the slope seems to be independent of the radiative heat flux from 50 to 30 kW/m².

In addition, the total heat release measured by $O_2$ consumption method (THR in MJ/m²) has been also calculated and compared to the value based on chemical heat of combustion (THR$_{max}$)[43] for PMMA (heat of combustion: 24.2 MJ/kg) and filled PVC (heat of combustion: 13.6 MJ/kg): for PMMA, 130 MJ/m² (THR at 21 vol.% $O_2$) very close to 129 MJ/m² (THR$_{max}$) and for filled PVC, 46.1 MJ/m² (THR at 21 vol.% $O_2$) with a difference to
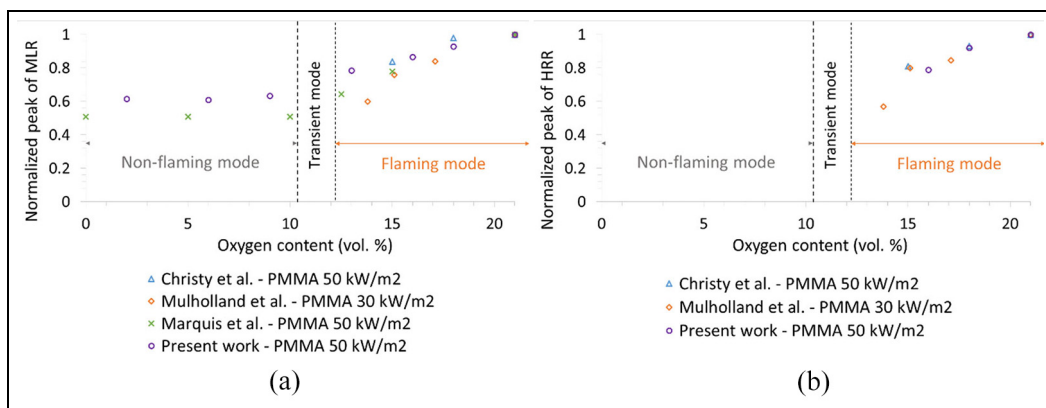
**Figure 8.** Comparison of the present work experimental values with the literature for (a) pMLR vs $O_2$ content and (b) pHRR vs $O_2$ content.

pHRR: peak of heat release rate; pMLR: peak of mass loss rate.

57.8 $MJ/m^2$ ($THR_{max}$), which could be related to the formation of a char residue and sample deformation, unlike PMMA, in CACC.

## Effect of vitiation on evolved gases

Figure 9 shows the evolution of evolved gases during PMMA burning at two $O_2$ contents. The temporal profiles of the velocity measured by Pitot tube in the 21 and 16 vol. % tests are close. So, direct comparisons of the concentration profiles obtained at different $O_2$ concentrations are made. It is seen that, considering the experimental uncertainties, the $O_2$ content seems to have no major effect on the $CO_2$, CO, $H_2O$, $CH_4$, $C_2H_4$, $C_2H_2$, and $C_6H_6$ production, which makes that the $[CO]/[CO_2]$ (v/v) ratio remains quite constant (around 0.1–0.2) regarding the vitiation in under-ventilated flaming fires. $CO_2$ is released at a concentration of approximately 60,000 ppmv and CO is released at a concentration peak of approximately 13,000 ppmv. $H_2O$ is released at a concentration of approximately 45,000 ppmv and $CH_4$, $C_2H_4$, $C_2H_2$, and $C_6H_6$ are released at a concentration peak of approximately 5000, 2200, 2000, and 800 ppmv.

Previously in Christy et al.,[22] it was observed that the effect of vitiation when varying $O_2$ content from 21 to 15 vol. % in well-ventilated conditions (1440 L/min of inlet flow rate) increases the $[CO]/[CO_2]$ (v/v) ratio of PMMA from 0.006 to 0.015. This trend is not observed in this present work because the vitiation effect is coupled with the under-ventilation effect. The insensitivity of both incomplete (CO, hydrocarbons) and complete ($H_2O$, $CO_2$) combustion product distributions to the $O_2$ content at the constant flow rate occurs because there is not enough oxygen in the combustion environment to complete the process. Indeed, the equivalence ratio is globally larger than 1, that is, fuel-rich flame, and is not in steady state during the tests.
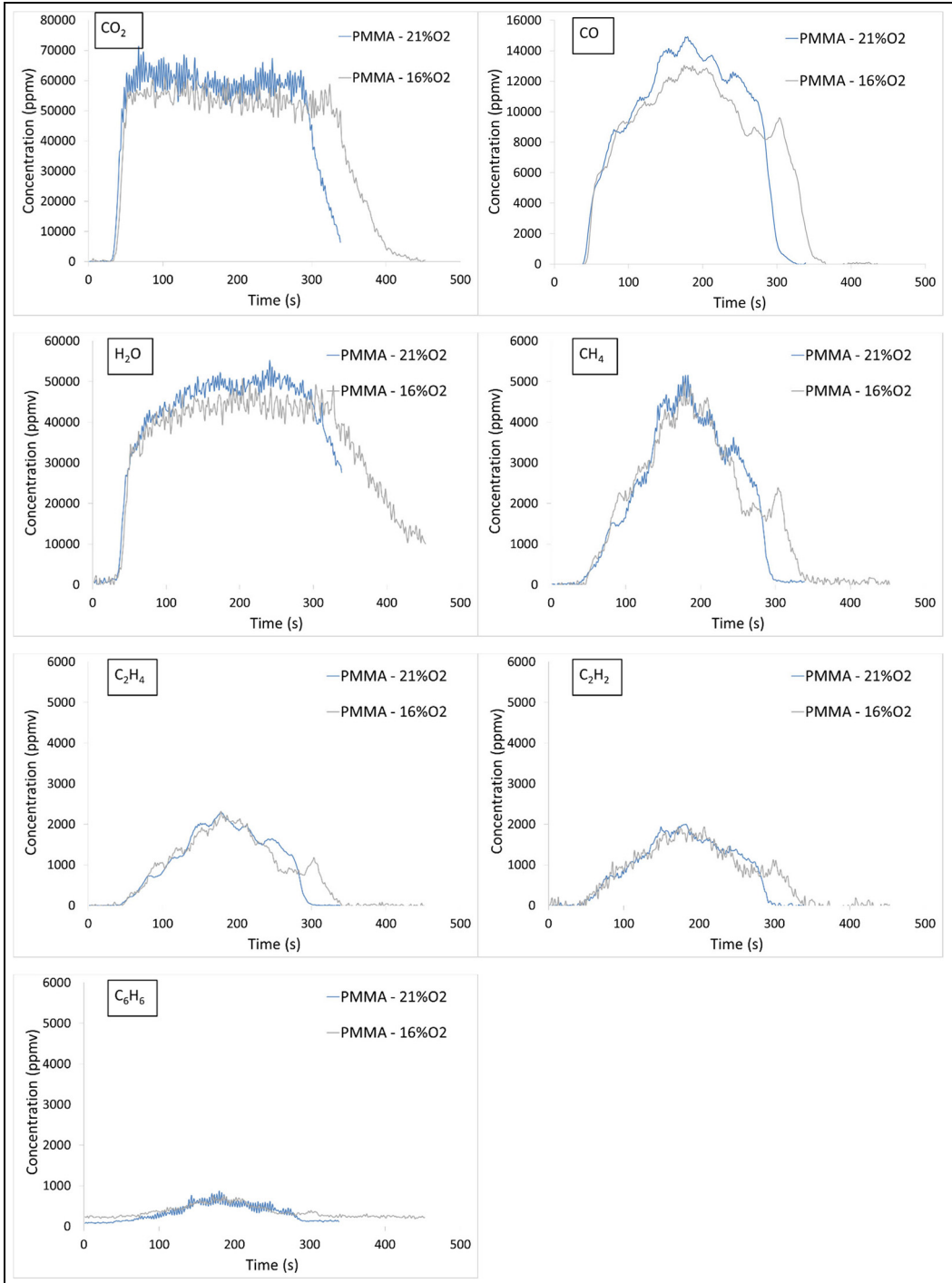
**Figure 9.** Evolution of evolved gases during PMMA burning at different $O_2$ contents in the inlet gas stream.
PMMA: polymethylmethacrylate.

Figure 10 shows the evolution of evolved gases of burning filled PVC at three $O_2$ contents. The $O_2$ content seems to have no effect on the $CO_2$, CO, $H_2O$, $CH_4$, $C_2H_4$, $C_2H_2$, $C_6H_6$, and HCl production, which makes the [CO]/[$CO_2$] ratio also independent of the $O_2$ content. $CO_2$ is released at a concentration peak of approximately 14,000 ppmv and CO is released at a concentration peak of approximately 2500 ppmv. $H_2O$ is released at a concentration of approximately 15,000 ppmv and $CH_4$, $C_2H_4$, $C_2H_2$, $C_6H_6$, and HCl are released at a concentration peak of approximately 300, 150, 200, 150, and 2500 ppmv.

### Effect of vitiation on evolved aerosols

Size classes from ELPI measurement expressed in number of particles are gathered in Figures 10 and 11 to provide readable data: total amount of particles (classes 1–14) in the left figure and focus on intermediate-sized particles (classes 7–9) from 0.257 to 0.603 μm in the right figure. Figure 11 shows the evolution of evolved aerosols during PMMA burning at three $O_2$ contents. The $O_2$ content seems to have no major effect on both the total amount of aerosols released and their size distribution. The total amount of evolved aerosols during under-ventilated and vitiated burning of PMMA exhibit a stationary phase of around $2.5 \times 10^8 \#/m^3$. At the end of the test during the HRR decreasing step, the high peaks observed for the total amount of particles could be related to the progressive extinction of the flame, generating aerosols.

Figure 12 shows the evolution of evolved aerosols of burning unfilled PVC at three $O_2$ contents. In our experimental conditions, the $O_2$ content has no major effect on both the total amount of aerosols released and their size distribution. The total amount of evolved aerosols during under-ventilated and vitiated burning of unfilled PVC is around $1.8 \times 10^8 \#/m^3$.

## Conclusion

A bench-scale CACC has been developed for studying oxygen-depleted fires. It is versatile equipment that permits to control several parameters such as the inlet gas composition, its inlet flow rate and distribution into the enclosure, and thus yields repeatable data. The results presented for PMMA and filled PVC have been obtained in under-ventilated (fuel-rich flame) and vitiated regime to get complementary data to observation obtained in the ventilated regime. The confrontation between the literature and the data obtained performing tests with PMMA evidence that this bench-scale apparatus is reliable and trustable. The original results obtained for filled PVC give an insight into the heat released and the species produced simultaneously during a fire in advanced stages. PMMA and PVC-based materials do not exhibit the same reaction toward under-ventilation and vitiation. PMMA exhibits a flame extinction transition around 13 vol. % $O_2$ whereas PVC-based material quench around 15 vol. % $O_2$. In the under-ventilated flaming regime, vitiation decreases the mass loss rate of both PMMA (−20% of pMLR between 21% and 13 vol. % $O_2$) and filled PVC (−17% of pMLR between 21% and 16 vol. % $O_2$) linearly. Vitiation lowers the heat release rate linearly in the case of PMMA burning (−20% of pHRR between 21 and 16 vol.% $O_2$), whereas it has no significant effect on the heat release rate in the case of PVC-based materials burning. However, vitiation in under-ventilated flaming regime has no major effect on the composition of gaseous species and the production of aerosols for both of the materials.
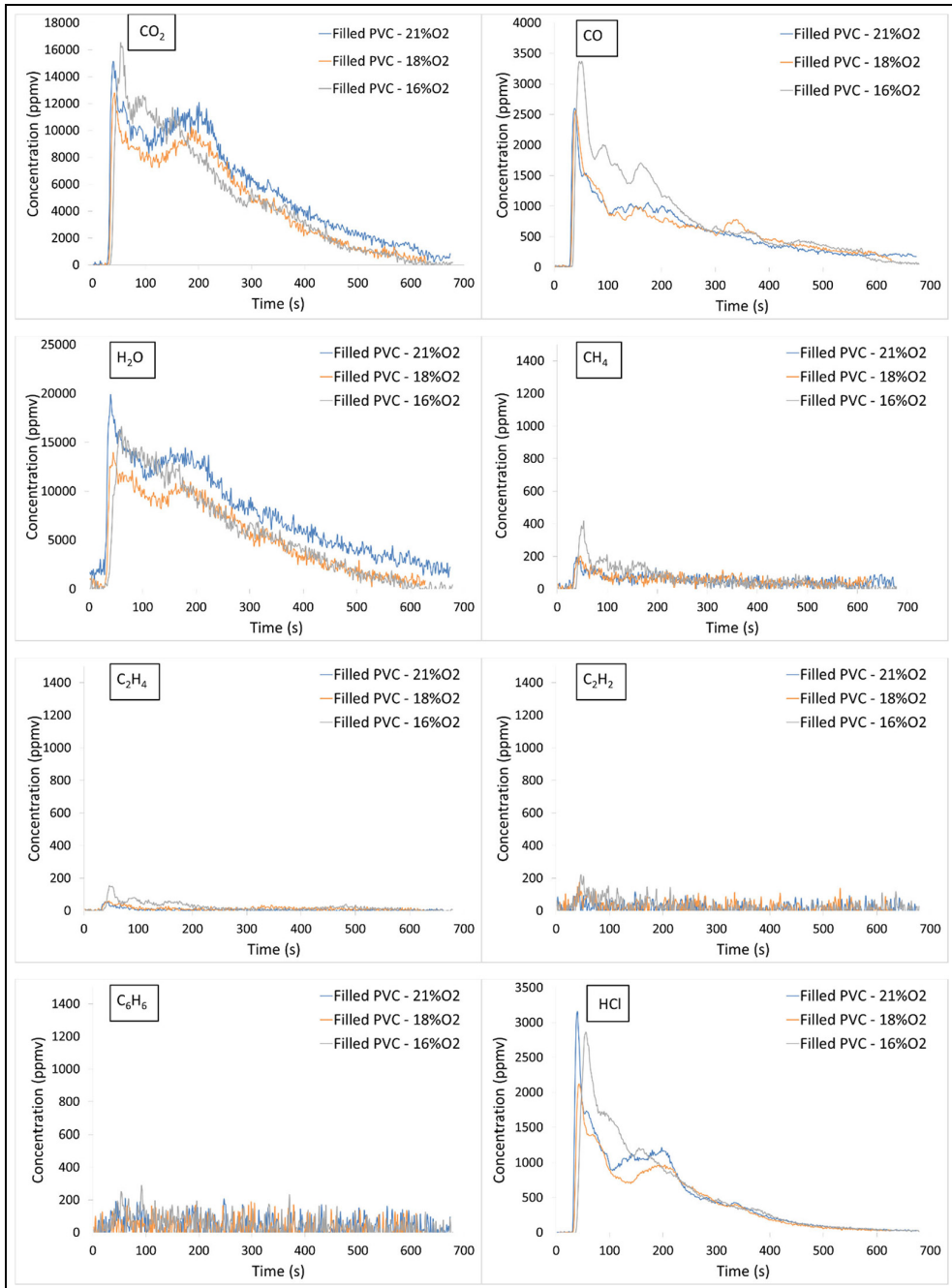
**Figure 10.** Evolution of evolved gases during filled PVC burning at different $O_2$ contents in the inlet gas stream.
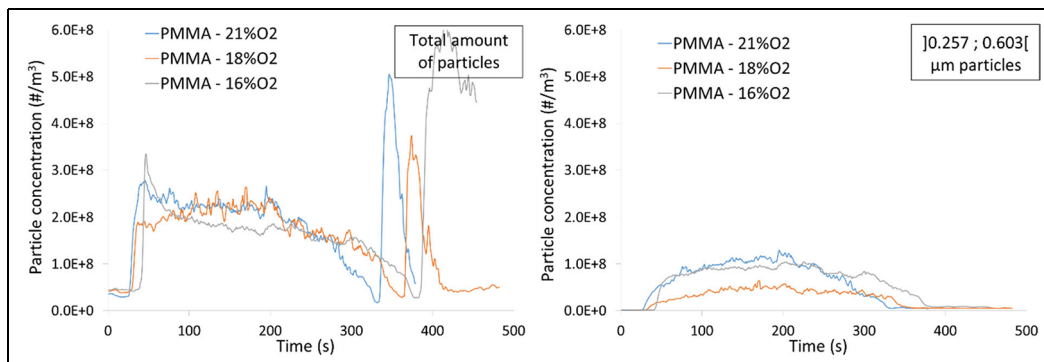PVC: polyvinylchloride.

**Figure 11.** Evolution of evolved aerosols during PMMA burning at different $O_2$ contents in the inlet gas stream (left: total amount of particles, right: particles of aerodynamic diameter 0.257–0.603 μm). PMMA: polymethylmethacrylate.
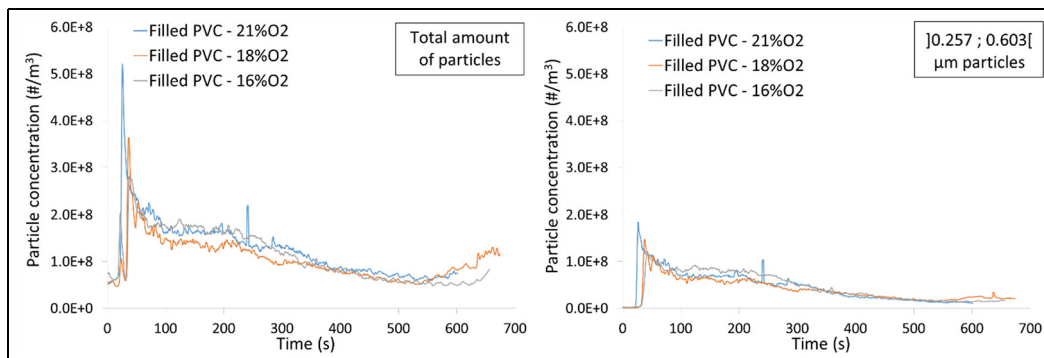


**Figure 12.** Evolution of evolved aerosols during filled PVC burning at different $O_2$ contents in the inlet gas stream (left: total amount of particles, right: particles of aerodynamic diameter 0.257–0.603 μm). PVC: polyvinylchloride.

## ORCID iDs

Olivier Authier ⓘ https://orcid.org/0000-0003-0662-0000
Serge Bourbigot ⓘ https://orcid.org/0000-0003-1536-2015
Gaëlle Fontaine ⓘ https://orcid.org/0000-0002-7113-1687

# References

1. Melis S and Audouin L. Effects of vitiation on the heat release rate in mechanically-ventilated compartment fires. *Fire Safety Sci* 2008; 9: 931–942.
2. Subudhi M. *Literature review of environmental qualification of safety-related electrical cables.* Report no. NUREG/CR-6384, vol. 1, part 1, April 1996. Upton, NY: Brookhaven National Laboratory.[AQ: 3]
3. Werrel M, Deubel JH, Krüger S, et al. The calculation of the heat release rate by oxygen consumption in a controlled-atmosphere cone calorimeter. *Fire Mater* 2014; 38: 204–226.
4. Standard test methods for measurement of synthetic polymer material flammability using a fire propagation apparatus (FPA), https://www.astm.org/e2058-13.html (accessed 13 January 2022).
5. NF P92-190-1; NF ISO 5660-1:2015. Reaction-to-fire tests—heat release, smoke production and mass loss rate—part 1: heat release rate (cone calorimeter method) and smoke production rate (dynamic measurement).
6. Standard test method for heat and visible smoke release rates for materials, and products using an oxygen consumption calorimeter, https://www.astm.org/e1354-17.html (accessed 13 January 2022).
7. Babrauskas V, Twilley WH, Janssens M, et al. A cone calorimeter for controlled-atmosphere studies. *Fire Mater* 1992; 16: 37–43.
8. ISO/TS 5660-5:2020(En). Reaction-to-fire tests—heat release, smoke production and mass loss rate—part 5: heat release rate (cone calorimeter method) and smoke production rate (dynamic measurement) under reduced oxygen atmospheres.
9. Marquis D, Guillaume E and Lesenechal D. Accuracy (trueness and precision) of cone calorimeter tests with and without a vitiated air enclosure. *Procedia Engineer* 2013; 62: 103–119.
10. Marquis DM, Hermouet F and Guillaume É. Effects of reduced oxygen environment on the reaction to fire of a poly(urethane-isocyanurate) foam: reaction to fire of PIR foam. *Fire Mater* 2017; 41: 245–274.
11. Fourneau C, Delvosalle C, Breulet H, et al. Characterization of highly under-ventilated fires using the cone calorimeter. *Fire Mater* 2016; 40: 434–444.
12. Barton J, Rios O, Runefors M, et al. The effect of oxygen concentration on selected industrial products in the open controlled atmosphere cone calorimeter. *Fire Mater.* Epub ahead of print 13 July 2021. DOI: 10.1002/fam.3006.
13. Beji T, Helson O, Rogaume T, et al. Experimental and numerical study on the evaporation rates of liquid fuels using a controlled atmosphere cone calorimeter. *Fire Safety J* 2021; 121: 103317.
14. Bray RJ, Barton J, Madsen D, et al. Burning material behaviour in hypoxic environments: an experimental study examining a representative storage arrangement of acrylonitrile butadiene styrene, polyethylene bubble wrap, and cardboard layers as a composite system. *Fire Mater* 2022; 46: 313–328.
15. Hermouet F, Rogaume T, Guillaume E, et al. Experimental characterization of the reaction-to-fire of an Acrylonitrile-Butadiene-Styrene (ABS) material using controlled atmosphere cone calorimeter. *Fire Safety J* 2021; 121: 103291.
16. ISO 12136:2011, https://www.iso.org/cms/render/live/en/sites/isoorg/contents/data/standard/05/12/51237.html (accessed 13 January 2022).
17. Stec AA, Hull TR, Lebek K, et al. The effect of temperature and ventilation condition on the toxic product yields from burning polymers. *Fire Mater* 2008; 32: 49–60.
18. Chatenet S, Lemesle M and Mongruel S. Enceinte de Sous-Ventilation Pour l'étude de la Décomposition Thermique en Atmosphère Contrôlée, 2018.[AQ: 4]
19. Tewarson A and Pion RF. Flammability of plastics—I. Burning intensity. *Combust Flame* 1976; 26: 85–103.
20. Santo G and Tamanini F. Influence of oxygen depletion on the radiative properties of PMMA flames. *Symp Int Combust* 1981; 18: 619–631.
21. Mulholland GW, Twilley WH, Babrauskas V, et al. The effect of oxygen concentration on CO and smoke produced by flames. *Fire Safety Science 1991*; 3: 585–594 (also published In: *Proceedings of the 3rd international symposium on fire safety science*, Edinburgh, 8–12 July 1991).
22. Christy MR, Petrella RV and Penkala JJ. Controlled-atmosphere cone calorimeter. In: Nelson GL (ed.) *Fire and polymers II*. Washington, DC: American Chemical Society, 1995.[AQ: 5]
23. Brohez S, Marlair G and Delvosalle C. The effect of oxygen concentration on CO and soot yields in fires. *Fire Mater* 2008; 32: 141–158.
24. Peatross MJ and Beyler CL. Ventilation effects on compartment fire characterization. *Fire Safety Sci* 1997; 5: 403–414.
25. Alibert D, Coutin M, Mense M, et al. Effect of oxygen concentration on the combustion of horizontally-oriented slabs of PMMA. *Fire Safety J* 2017; 91: 182–190.
26. Marquis D, Guillaume E and Camillo A. Effects of oxygen availability on the combustion behaviour of materials in a controlled atmosphere cone calorimeter. *Fire Safety Sci* 2014; 11: 138–151 (also published In: *Proceedings of the 11th international symposium on fire safety science*, Christchurch, New Zealand, 10–14 February 2014).
27. Tewarson A, Jiang FH and Morikawa T. Ventilation-controlled combustion of polymers. *Combust Flame* 1993; 95: 151–169.
28. Hietaniemi J, Kallonen R and Mikkola E. Burning characteristics of selected substances: production of heat, smoke and chemical species. *Fire Mater* 1999; 23: 171–185.
29. Fourneau C, Delvosalle C, Breulet H, et al. Study of under-ventilated burning characteristics of materials with the cone calorimeter. *Chem Engineer Trans* 2013; 31: 871–876.
30. Ngohang FE, Fontaine G, Gay L, et al. Revisited investigation of fire behavior of ethylene vinyl acetate/aluminum trihydroxide using a combination of mass loss cone, Fourier transform infrared spectroscopy and electrical low pressure impactor. *Polym Degrad Stabil* 2014; 106: 26–35.
31. Ngohang FE, Fontaine G, Gay L, et al. Smoke composition using MLC/FTIR/ELPI: application to flame retarded ethylene vinyl acetate. *Polym Degrad Stabil* 2015; 115: 89–109.
32. Fontaine G, Ngohang FE, Gay L, et al. Investigation of the contribution to fire of electrical cable by a revisited mass loss cone. In: Harada K, Matsuyama K, Himoto K, et al. (eds) *Fire science and technology 2015*. Singapore: Springer, 2017, pp. 687–693.
33. Huggett C. Estimation of rate of heat release by means of oxygen consumption measurements. *Fire Mater* 1980; 4: 61–65.
34. Parker WJ. *Calculations of the heat release rate by oxygen consumption for various applications.* NBSIR 81-2427-1, March 1982. Washington, DC: National Bureau of Standards.[AQ: 6]
35. Janssens ML. Measuring rate of heat release by oxygen consumption. *Fire Technol* 1991; 27: 234–249.

36. Järvinen A, Aitomaa M, Rostedt A, et al. Calibration of the new electrical low pressure impactor (ELPI + ). *J Aerosol Sci* 2014; 69: 150–159.

37. Association Française de Normalisation (AFNOR) NF—ISO 19706:2011-11. Lignes Directrices Pour l'évaluation des Dangers du feu Pour les Personnes.

38. Pitts WM. The global equivalence ratio concept and the formation mechanisms of carbon monoxide in enclosure fires. *Prog Energ Combust* 1995; 21: 197–237.

39. Patel P, Hull TR and Stec AA. Influence of physical properties on polymer flammability in the cone calorimeter. *Polym Advan Technol* 2011; 22: 1100–1107.

40. Tewarson A, Lee JL and Pion RF. The influence of oxygen concentration on fuel parameters for fire modeling. In: *Proceedings of the 18th symposium (international) on combustion*, Waterloo, ON, Canada, 17–22 August 1980.

41. Kashiwagi T and Ohlemiller TJ. A study of oxygen effects on non flaming transient gasification of PMMA and PE during thermal irradiation. In: *Proceedings of the 19th symposium (international) on combustion*, Haifa, Israel, 8–13 August 1982, pp. 815–823. Pittsburgh, PA: The Combustion Institute.

42. Kashiwagi T. Polymer combustion and flammability—role of the condensed phase. *Symp Int Combust* 1994; 25: 1423–1437 (also published In: *Proceedings of the 25th symposium (international) on combustion*, Irvine, CA, 31 July–5 August 1994).

43. Tewarson A. Chapter 4: generation of heat and chemical compounds in fires. In: DiNenno PJ (ed.) *SFPE handbook of fire protection engineering*, vol. section 3. Berlin: Springer Nature, 1995, pp. 3–53 to pp. 3–124.

## Author biographies

[AQ: 2]